



cal shift changes are an indication of variations in the O-P-O bond angle or torsion angles along the nucleic acid phosphodiester backbone.

**Nuclear Overhauser effect (17, 18).** The proton nuclear Overhauser effect (NOE) is a distance-measuring probe of conformation and corresponds to a change in the resonance intensity of a given proton spin on saturation of a nearby dipolar coupled proton spin. (Saturation corresponds to the application of an on-resonance radio-frequency pulse that equalizes the spin population between states, resulting in loss of the resonance signal.) The magnitude and sign of NOE effects between proton spins depend on the inverse sixth power of the distance between the protons and on the frequency of motions of the spins. NOE effects are negative for nucleic acids at the dodecanucleotide duplex level, corresponding to a decrease in intensity ranging from a few percent at interproton distances of 3.5 angstroms to much larger perturbations at shorter distances. NOE effects are best represented as the difference between on- and off-resonance spectra, in which the intensity perturbations can be readily detected along with the strong signal of the saturated resonance.

**Line widths.** The width of a nucleic

Table 1. Watson-Crick imino proton chemical shifts in the dodecamer, tridecamer, and dodecamer GT duplexes at  $-5^{\circ}\text{C}$ .\*

| Resonance | Assignment | Chemical shift (ppm) |            |              |
|-----------|------------|----------------------|------------|--------------|
|           |            | Dodecamer            | Tridecamer | Dodecamer GT |
| G(H-1)    | 1          | 13.29                | 13.32      | 13.26        |
| G(H-1)    | 2          | 13.14                | 13.19      | 13.21        |
| G(H-1)    | 3          | 12.96                | 13.00      | 10.58†       |
| G(H-1)    | 4          | 12.75                | 12.39      | 12.97        |
| T(H-3)    | 5          | 13.97                | 13.90      | 13.82        |
| T(H-3)    | 6          | 13.86                | 13.78      | 13.82        |

\*Buffer: 0.1M phosphate, 2.5 mM EDTA, 4:1  $\text{H}_2\text{O}:\text{D}_2\text{O}$ , pH  $7.5 \pm 0.2$ . †The T(H-3) proton resonates at 11.78 ppm in the dG:dT pair.

acid NMR resonance reflects the magnetic spin-spin interactions with nearby protons and nitrogen and phosphorus nuclei and the contribution from chemical kinetic processes. For CH protons, which do not exchange with solvent water, increases in line width are observed when the conformational interconversion rate between duplex and strands is on the order of the chemical shift separation between corresponding proton resonances in each state. For exchangeable NH and OH protons, the excess line width contributions reflect exchange rates with solvent water and are a mea-

sure of the relative stability of the local duplex structure. The exchangeable resonances broaden out when their exchange rates with solvent water approach 200 per second.

**Saturation recovery (17, 18).** The recovery of magnetization following saturation of an exchangeable resonance can be monitored by incorporating a variable time delay between the saturation and observation pulses in a Fourier transform NMR experiment. [The Redfield 214-pulse sequence (17, 18) is used to null the strong  $\text{H}_2\text{O}$  resonance of the solvent.] The magnetization recovers by spin lattice relaxation and by chemical exchange with unperturbed solvent water. The former process predominates at low temperatures and has a small activation energy. By contrast, solvent exchange rates have a large temperature dependence and generally predominate above room temperature for oligonucleotide duplexes. The saturation recovery method is useful for evaluating exchange rates greater than  $5 \text{ sec}^{-1}$  and measures rate changes over two orders of magnitude.

The power of the NOE and saturation transfer methodology was elegantly demonstrated by Redfield and co-workers (17, 18) in their seminal NMR investigation of the structure and dynamics of transfer RNA in solution.

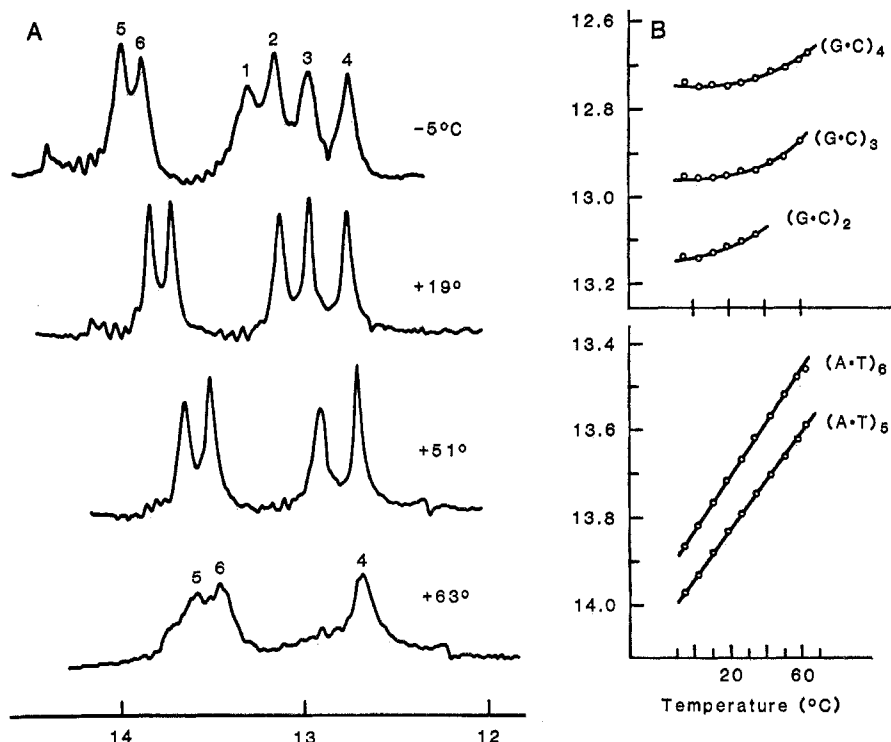


Fig. 1. (A) The 360-MHz correlation proton NMR spectra (12 to 14 ppm) of the dodecamer duplex in 0.1M phosphate, 2.5 mM EDTA, 4:1  $\text{H}_2\text{O}:\text{D}_2\text{O}$ , pH 7.50, between  $-5^{\circ}\text{C}$  and  $+63^{\circ}\text{C}$ . The signal-to-noise ratios of the spectra were improved by applying a 5-Hz exponential line-broadening contribution. The imino proton assignments are designated over the resonances. (B) Temperature dependence of the chemical shifts of the five nonterminal imino protons of the dodecamer duplex in the buffer solution described above.

#### d(CGCGAATTCGCG) Dodecamer Duplex

The d(CGCGAATTCGCG) sequence (1) is the first oligonucleotide duplex containing at least one turn of helix for which x-ray (20, 21) and NMR (22) information is available. This permits a detailed comparison of the structure and dynamics of a dodecanucleotide in heavily hydrated crystals at atomic resolution and during the premelting and melting transitions in aqueous solution.

**Symmetry.** The Watson-Crick imino protons (guanosine H-1 in a dG:dC pair and thymidine H-3 in a dA:dT pair) resonate between 12 and 15 parts per million (ppm) in  $\text{H}_2\text{O}$  solution (23) and have been extensively used to estimate the number and stability of base pairs in nucleic acid duplexes (16). We observe six imino protons in the spectrum of the dodecamer at  $-5^{\circ}\text{C}$  (Fig. 1A), consistent with formation of a 12-base pair self-complementary duplex with a twofold element of symmetry. In contrast, exact twofold symmetry is not observed in the dodecamer crystal (20, 21), presumably due to contributions from packing forces in the solid state.

**Fraying.** The resonances of the imino protons of the four dG·dC base pairs between 12.7 and 13.3 ppm broaden out in a sequential manner with increasing temperature in the dodecamer spectrum in 0.1 molar phosphate solution at pH 7.5 (Fig. 1A). The decrease in lifetime of these exchangeable imino protons reflects the rapid opening and closing of base pairs at the ends of the duplex in the premelting transition region. The sequential broadening of the resonances of the dG·dC imino protons from the ends of the duplex readily permits their identification in the dodecamer sequence. The exchange of imino protons through a fraying process (24) is catalyzed by base (25), and we observe the predicted increase in line widths at higher pH values at a fixed temperature.

It should be noted that the imino protons of base pairs 1, 2, and 3 in the dodecanucleotide duplex exhibit exchange rates greater than  $200 \text{ sec}^{-1}$  below  $60^\circ\text{C}$ , and the resultant broadening (Fig. 1A) occurs below the temperature of  $72^\circ\text{C}$  at the midpoint of the duplex-to-strand transition in 0.1M buffer solution.

The imino protons of dA·dT base pairs 5 and 6 (spectral region 13.8 to 14.0 ppm) were differentiated by the observation of a small negative NOE (17, 18) between the downfield resonance in the pair and the known imino proton of dG·dC base pair 4 at 12.75 ppm. The ability to observe and assign (Fig. 1A and Table 1) all six imino protons provides unique markers distributed throughout the length of the dodecamer duplex in solution.

**Premelting conformational transition.** The temperature-dependent chemical shifts of the five nonterminal imino protons of the dodecamer are plotted in Fig. 1B and show striking differences between the dA·dT and dG·dC base pairs. Both thymidine imino protons located in the center of the duplex exhibit a large linear temperature-dependent upfield shift, which is not observed at the guanine imino protons of the flanking dG·dC base pairs (Fig. 1B). The observed temperature-dependent premelting conformational transition at the central dA·dT tetranucleotide segment may reflect changes in the winding of the duplex or changes in the extent of propeller-twisting of the base pairs in the core of the duplex.

The x-ray investigations show that the d(CGCGAATTCGCG) duplex can adopt different right-handed conformations, depending on the temperature and on the alcohol concentration of the crystallization medium (26). These dodecanucleotide structures differ in the extent of base

Table 2. Lifetimes (milliseconds) of imino protons in the dodecamer, tridecamer, and dodecamer GT duplexes in 0.1M phosphate, pH 6,  $35^\circ\text{C}$ .

| Duplex       | Base pair |     |     |     |
|--------------|-----------|-----|-----|-----|
|              | 3         | 4   | 5   | 6   |
| Dodecamer    | 130       | 170 | 140 | 230 |
| Tridecamer   | *         | 62  | 100 | 160 |
| Dodecamer GT | 11,11     | 90  | 135 | 230 |

\*The lifetime is too short to observe at this temperature.

pair propeller twists and minor groove widths in the central d(AATT) segment. Thus the NMR and x-ray studies independently demonstrate that the premelting transition is localized at the internal dA·dT-rich segment of the duplex.

**Duplex opening rates.** Johnston and Redfield (27, 28) developed a saturation recovery method for measuring the exchange rates of individual imino protons in nucleic acid duplexes with solvent water. The recovery rate following saturation of the imino protons is the sum of the magnetic cross-relaxation rate with adjacent proton spins and the exchange rate with solvent. The temperature dependence of the lifetimes of the thymidine imino protons of base pairs 5 and 6 in the dodecamer duplex in 0.1M phosphate at pH 6 is plotted in Fig. 2A, and

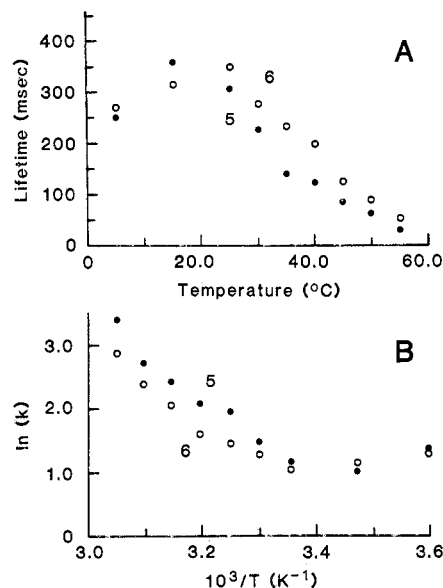
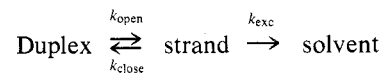


Fig. 2. (A) Temperature dependence of the observed lifetimes for the two thymidine imino protons of base pairs 5 and 6 on the dodecamer duplex in 0.1M phosphate, 2.5 mM EDTA, 4:1 H<sub>2</sub>O:<sup>2</sup>H<sub>2</sub>O, pH 6.0. The thymidine imino protons of base pairs 5 and 6 are represented by (●) and (○), respectively. (B) Arrhenius plot for the observed lifetimes of the thymidine imino protons of the dodecamer, from which the activation energies described in the text were obtained. Conditions and symbols are the same as those given in (A).

the exchange contribution to these lifetimes dominates the high-temperature data (27–29).

Exchange of imino protons in nucleic acid duplexes with solvent water (30, 31) can be schematically represented by



where  $k_{\text{exc}}$  is the exchange rate constant. The exchange occurs from the strand state in this model, and the specific mechanism depends on the competition between  $k_{\text{close}}$  and  $k_{\text{exc}}$ . When  $k_{\text{exc}} \gg k_{\text{close}}$ , exchange with solvent occurs every time the duplex opens and the exchange process is a measure of the helix opening rates (25, 30, 31).

The lifetimes for opening individual imino protons in their respective internal base pairs for the dodecamer duplex at  $35^\circ\text{C}$  are summarized in Table 2. We note that under these conditions the lifetime increases from 130 milliseconds at base pair 3 to 230 milliseconds at base pair 6, which is farther into the interior of the duplex. The pH independence of the exchange lifetimes listed in Table 2 is consistent with the idea that the exchange rates provide a measure of the helix lifetime in the interior of the duplex.

**Individual base pair opening.** The temperature dependence of the exchange contribution to the transfer rates at the thymidine imino protons of base pairs 5 and 6 in the central core of the dodecamer duplex is given in an Arrhenius plot in Fig. 2B. The high-temperature rates are dominated by exchange and yield activation energies of  $14 \pm 2$  kilocalories at each position. This demonstrates that imino proton exchange in the interior of duplexes occurs by transient opening of individual dA·dT base pairs without disruption of adjacent base pair regions. The measured activation energy is in excellent agreement with corresponding values for opening barriers deduced from hydrogen-deuterium stopped-flow measurements of poly(A)·poly(U) (32) and NMR relaxation measurements on dA·dT base pairs in DNA restriction fragments (33).

**Nonexchangeable base protons.** We observe well-resolved nonexchangeable protons in the resolution-enhanced 500-megahertz spectrum of the aromatic region (7.0 to 8.1 ppm) of the dodecamer duplex at ambient temperature (Fig. 3A). The resonances have been assigned to specific positions on the purine and pyrimidine rings on the basis of their splitting patterns (pyrimidine H-6 and H-5 are doublets; thymidine H-6 singlets are broad due to long-range coupling to CH<sub>3</sub>-

5 resonances), susceptibility to deuteration at high temperature (guanosine H-8 is more readily deuterated than adenosine H-8), and differential spin lattice relaxation times (adenosine H-2 is distant from the sugar protons and exhibits long relaxation times). The assignment of a particular type of resonance to a specific base pair in the dodecamer sequence was achieved by chemical modification and NOE experiments (34). The chemical shift assignments of the dodecamer nonexchangeable protons at ambient temperature are listed in Table 3.

**Cooperative melting transition.** The nonexchangeable base proton resonances shift as average peaks during the dodecamer helix-coil transition with the experimental data for the four dG-dC base pairs plotted in Fig. 3B. The nonexchangeable protons distributed throughout base pairs 2, 3, 4, 5, and 6 exhibit a common transition midpoint of  $72^\circ \pm 2^\circ\text{C}$  in 0.1M phosphate solution (Table 3). This result demonstrates that at least of ten nonterminal base pairs in the dodecamer duplex melt in a cooperative manner during the helix-coil transition.

**Stacking in the crystalline and solution states.** We observe upfield shifts at all the dodecanucleotide base protons on duplex formation with magnitudes that vary widely with position in the dodecamer sequence (Table 3). Sarma and co-workers (35) computed the upfield chemical shifts for these protons on the basis of ring current and magnetic anisotropy contributions (36) for the overlap geometry observed in the dodecanucleotide

crystal (21). These calculated shifts are listed in Table 3, and one observes a good correlation with the experimental shifts at base pairs 3, 4, 5, and 6 in the dodecamer sequence. This suggests that the overlap geometry of the central octanucleotide segment observed in the crystal structure of the d(CGCGAATTCGCG) duplex (21) is retained in solution.

The discrepancies between the experimental and calculated shifts at base pairs 1 and 2 at either end of the dodecamer duplex may reflect contributions from crystal packing forces involving the mutual interaction of trinucleotide ends of adjacent molecules in the crystalline state (20, 21), which do not occur in solution (22).

**Phosphodiester backbone.** We observe partially resolved phosphodiester resonances in the  $^{31}\text{P}$  NMR spectra of the dodecamer duplex in the absence and presence of 5M NaCl solution at  $\sim 43^\circ\text{C}$  (Fig. 4A). The 0.45 ppm chemical shift dispersion in the absence of salt (top spectrum in Fig. 4A) increases to a 0.8 ppm dispersion on the addition of a high salt concentration (bottom spectrum in Fig. 4A). The dispersion decreases to 0.25 ppm in the dodecamer strand state at a high temperature. These results are indicative of sequence-dependent variations in either the O-P torsion angles or the O-P-O bond angles in the duplex state (37-39). We are unable to assign individual resonances to specific phosphodiester in the dodecanucleotide duplex at this time.

**Right-handed duplex.** We previously observed phosphorus resonances of

equal area at  $\sim 3.0$  and  $\sim 4.4$  ppm on formation of a left-handed dinucleotide repeat conformation of the  $(\text{dG-dC})_n$  duplex in high-salt solution (40). The absence of any phosphodiester resonance at  $\sim 3.0$  ppm in the  $^{31}\text{P}$  NMR spectra of the dodecamer as a function of salt concentration (Fig. 4A) is consistent with the formation of a right-handed dodecanucleotide duplex in low- and high-salt solution.

Thus the d(CGCG) alternating purine-pyrimidine ends of the d(CGCGAATTCGCG) duplex are unable to switch to the left-handed dinucleotide repeat conformation in the crystalline (20) and solution (22) states due to the presence of an intervening nonalternating d(AATT) segment. Future efforts should be directed toward the d(CGCGTATACGCG) duplex and its 2-aminoadenosine analogs in an attempt to determine whether the alternating dG-dC tetranucleotide blocks can switch the alternating dA-dT tetranucleotide block to a left-handed Z-DNA helix.

#### d(CGCGAATTCGCG) Tridecamer Duplex

The reading frame of the triplet genetic code can be dramatically altered by the insertion or deletion of a single base in one strand of the DNA duplex. It is imperative that such helix interruptions be readily recognized by repair enzymes, and we were interested in deducing the conformational features of such helix imperfections in the double helix.

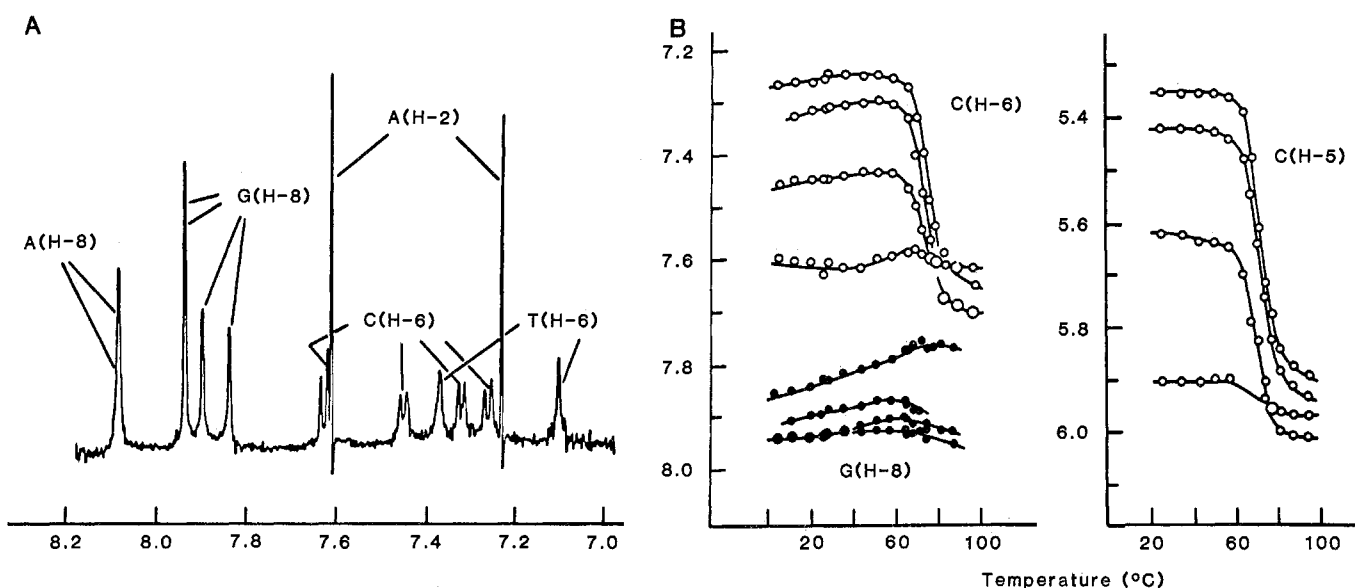


Fig. 3. (A) The 500-MHz Fourier transform proton NMR spectra (7.0 to 8.1 ppm) of the dodecamer duplex in 0.1M phosphate, 2.5 mM EDTA,  $^2\text{H}_2\text{O}$ , pH 7.70, at ambient temperature. The resolution of the spectrum was improved by applying an exponential line-narrowing contribution. (B) Temperature-dependent 360-MHz chemical shifts of the guanidine H-8 and cytosine H-6 and H-5 resonances of the dodecamer duplex in the buffer solution described above.



extended phosphodiester linkages at the DNA binding sites of intercalating agents (15, 42).

Extension of these studies to the d(CGCTGAATTCGCG) duplex, which contains an extra thymidine between positions 3 and 4, should reveal whether the extra pyrimidine base stacks into the helix or loops out into the solution.

### d(CGCTGAATTCGCG) Dodecamer

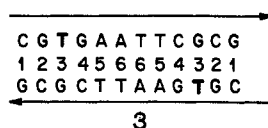
#### GT Duplex

Spontaneous substitution mutations during DNA replication can result in noncomplementary base pair formation. Topal and Fresco (43) considered alternate pairing modes by invoking imino or enol base tautomers including protonated species, as well as *syn* isomers about the glycosidic bond. NMR is ideally suited to probe the formation of these unfavored base-pairing interactions and deduce the extent of conformational change that would have to be recognized by the DNA polymerase during the proofreading process.

Crick (44) originally introduced the wobble hypothesis to account for the interaction between messenger RNA codon and transfer RNA anticodon. He noted that standard Watson-Crick base pairs are mandatory at the first two positions in the triplet but that there could be

more than one type of pairing at the third position. This results in a certain amount of play or wobble, so that the formation of G·A, G·U, C·U, and U·U wobble pairs can explain the general nature of the degeneracy of the genetic code.

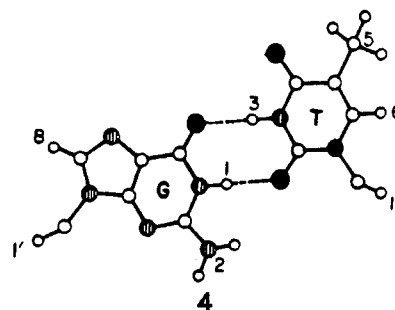
We initiated a study of the structure and dynamics of noncomplementary base-base interactions in the interior of nucleic acid duplexes. Our early efforts were focused on the dG·dT interaction, since this type of mismatch is a common feature in the stem regions of transfer and ribosomal RNA structures (17). Crick (44) proposed that dG·dT or G·U forms a wobble base pair in which the purine and pyrimidine rings are displaced relative to each other to form two imino-carbonyl hydrogen bonds. We report below on the d(CGCTGAATTCGCG) dodecamer GT duplex (3), which con-



tains two non-Watson-Crick dG·dT interactions at position 3 from each end of the duplex (45). The NMR research focuses on the conformational and dynamic features at and adjacent to the mispairing site in the dodecamer GT duplex in solution.

*Wobble pair formation.* The exchangeable proton NMR spectrum of the dodec-

amer GT duplex shows the imino protons of dA·dT base pairs 5 and 6 at 13.7 ppm; dG·dC base pairs 1, 2, and 4 between 12.9 and 13.2 ppm; and two new resonances at 10.55 and 11.65 ppm at 5°C (top spectrum in Fig. 6A). The latter resonances are assigned to the guanosine and thymidine imino protons in the dG·dT interaction, and their upfield shift relative to the remaining imino protons reflects formation of intramolecular hydrogen bonds with carbonyl groups in the wobble pair (4) rather than with ring nitrogens in the Watson-Crick pair.



The NOE difference spectrum following saturation of the 10.55-ppm dG·dT imino proton at position 3 in the dodecamer GT duplex at 5°C is shown at the bottom in Fig. 6A. We observe a 36 percent negative NOE at the 11.65-ppm dG·dT imino proton at position 3, consistent with the close proximity of the guanosine and thymidine imino protons in the wobble pair (4). In addition, small-

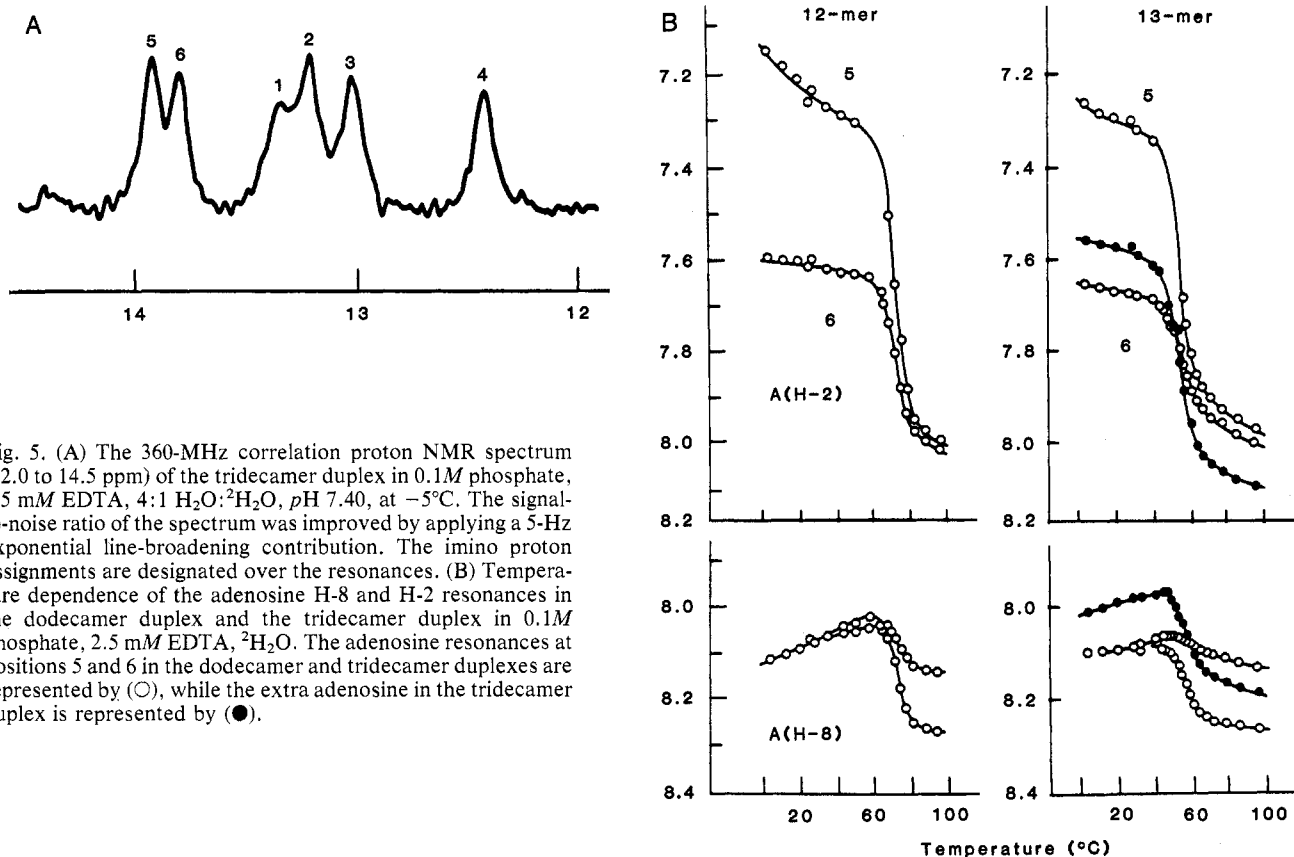


Fig. 5. (A) The 360-MHz correlation proton NMR spectrum (12.0 to 14.5 ppm) of the tridecamer duplex in 0.1M phosphate, 2.5 mM EDTA, 4:1 H<sub>2</sub>O:<sup>2</sup>H<sub>2</sub>O, pH 7.40, at -5°C. The signal-to-noise ratio of the spectrum was improved by applying a 5-Hz exponential line-broadening contribution. The imino proton assignments are designated over the resonances. (B) Temperature dependence of the adenosine H-8 and H-2 resonances in the dodecamer duplex and the tridecamer duplex in 0.1M phosphate, 2.5 mM EDTA, <sup>2</sup>H<sub>2</sub>O. The adenosine resonances at positions 5 and 6 in the dodecamer and tridecamer duplexes are represented by (○), while the extra adenosine in the tridecamer duplex is represented by (●).

er negative NOE's of 16 and 15 percent are observed at the imino protons of dG·dC Watson-Crick base pairs 2 and 4, which are on either side of the wobble base pair at position 3 in the dodecamer GT duplex (bottom spectrum in Fig. 6A). These results and earlier investigations of transfer RNA by Roy and Redfield (46) show that it is possible to observe NOE's between imino protons on adjacent base pairs separated by  $\sim 3.4 \text{ \AA}$  and introduce a powerful new approach to resonance assignments (46, 47).

**Exchange characteristics.** The resonances of both imino protons in the wobble pair in the dodecamer GT duplex broaden to the same extent when the temperature is raised to 35°C, demonstrating that exchange of the dG·dT guanosine and thymidine imino protons occurs by a common pathway. This supports an earlier suggestion that base pair opening is a prerequisite for the exchange of imino protons in oligonucleotide duplexes in solution (32).

The exchange of both imino protons in the dG·dT wobble pair at position 3 exhibits lifetimes of 11 msec each in the dodecamer GT duplex at 35°C, compared to 130 msec for the dG·dC Watson-Crick base pair at position 3 in the dodecamer duplex at the same temperature (Table 2). The order of magnitude difference in opening rates reflects the destabilization of a dG·dT base pair relative to a dG·dC base pair in the interior of the duplex.

**Stacking at the wobble site.** The non-exchangeable thymidine H-6 and CH<sub>3</sub>-5

protons in the wobble pair can be distinguished from the thymidines at positions 5 and 6 in the dodecanucleotide duplex by comparing the temperature-dependent thymidine chemical shifts in the dodecamer and dodecamer GT duplexes (Fig. 6B). The thymidine H-6 proton in the wobble pair can be readily identified from its unique chemical shifts in the duplex and strand states.

The magnitude of the pyrimidine H-6 upfield shift is smaller for the thymidine at position 3 (0.24 ppm) in the dodecamer GT duplex than for the cytidine at position 3 (0.4 ppm) in the dodecamer duplex. These results indicate that the thymidine is displaced on formation of the wobble base pair so that it stacks to a lesser degree with adjacent base pairs in the dodecamer GT duplex compared to a Watson-Crick base-paired cytidine at the same position in the dodecamer duplex.

We measure a common transition midpoint of  $52^\circ \pm 2^\circ\text{C}$  at the base protons of dG·dC base pairs 2 and 4, wobble base pair 3, and dA·dT base pairs 5 and 6 in the dodecamer GT duplex, indicating a 20°C destabilization when the two Watson-Crick dG·dC base pairs are replaced by two wobble dG·dT base pairs at the dodecanucleotide duplex level.

**Localization of wobble conformational change.** The imino protons of dG·dC base pairs 2 and 4 are readily observable between 12.9 and 13.2 ppm in the dodecamer GT spectrum at 5°C (Fig. 6A), indicating intact base pairing adjacent to the wobble mispairing site at low tem-

perature. The lifetimes for opening of base pairs 4, 5, and 6 in the dodecamer and dodecamer GT duplexes in 0.1M phosphate, pH 6, at 35°C are summarized in Table 2. Replacement of a dG·dC Watson-Crick pair at position 3 by a dG·dT wobble pair results in a twofold decrease in the helix opening lifetime at adjacent position 4 but no change at dA·dT base pairs 5 and 6. The NMR results demonstrate that the introduction of wobble pairs at position 3 results in a conformational perturbation that is localized at adjacent dG·dC base pairs and does not extend into the interior of the dodecanucleotide duplex.

**Phosphodiester linkage at wobble site.** The phosphodiester resonances are resolved over an 0.84-ppm chemical shift dispersion in the dodecamer GT duplex at 15°C in aqueous solution (Fig. 4C). A comparison of the phosphorus spectra of the dodecamer duplex in the absence of added salt (top spectrum in Fig. 4A) and the dodecamer GT duplex (Fig. 4C) suggests that the resolved phosphates downfield (at 3.80 ppm) and upfield (at 4.64 ppm) of the main cluster should be tentatively assigned to the phosphodiester at the wobble site in the dodecamer GT duplex in solution.

Extension of these investigations to the d(CGCGTGTGCGCG) sequence, which has four dG·dT interactions in the center of the duplex, is of interest. It is conceivable that this dodecanucleotide may undergo a biphasic melting transition with the middle opening before the ends of the duplex.

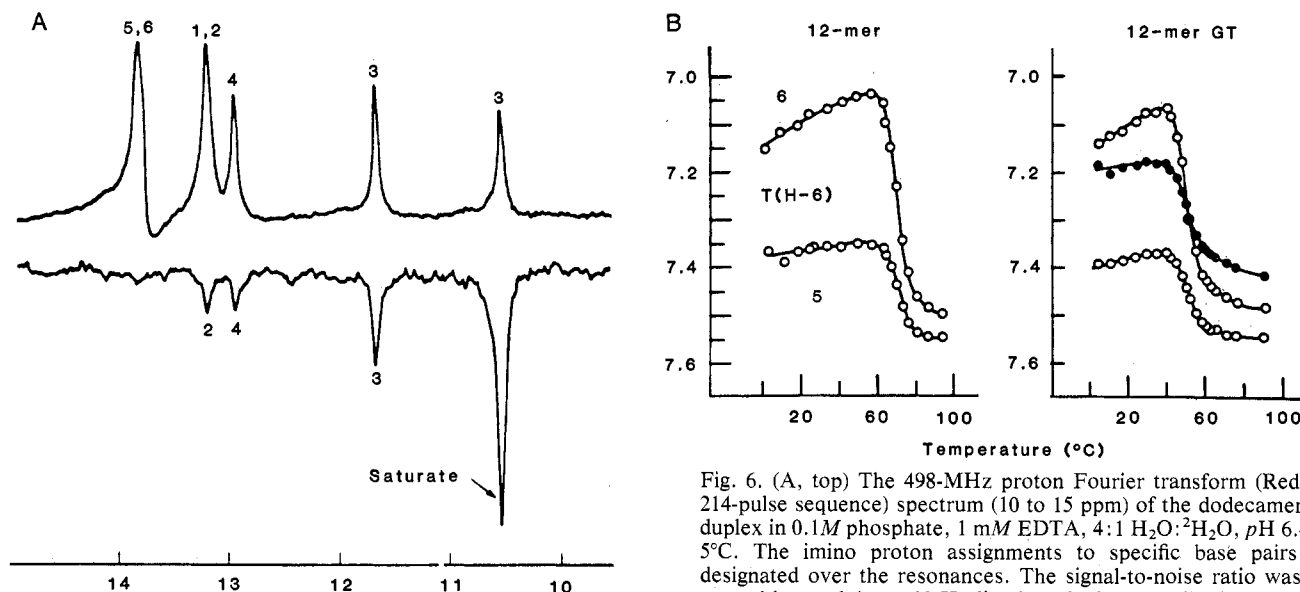


Fig. 6. (A, top) The 498-MHz proton Fourier transform (Redfield 214-pulse sequence) spectrum (10 to 15 ppm) of the dodecamer GT duplex in 0.1M phosphate, 1 mM EDTA, 4:1 H<sub>2</sub>O:<sup>2</sup>H<sub>2</sub>O, pH 6.4, at 5°C. The imino proton assignments to specific base pairs are designated over the resonances. The signal-to-noise ratio was improved by applying a 10-Hz line-broadening contribution. (A, bottom) Difference spectrum following saturation of the 10.55 ppm imino proton of wobble pair 3 in the dodecamer GT duplex. Negative NOE's are observed at the other imino proton of wobble pair 3 at 11.65 ppm (36 percent) and the imino protons of Watson-Crick base pair 2 at 13.13 ppm (16 percent) and base pair 4 at 12.89 ppm (15 percent) in the dodecamer GT duplex. (B) Temperature dependence of the thymidine H-6 resonances in the dodecamer duplex and the dodecamer GT duplex in 0.1M phosphate, 2.5 mM EDTA, <sup>2</sup>H<sub>2</sub>O. The thymidine resonances at positions 5 and 6 in the dodecamer and dodecamer GT duplexes are represented by (○), and the thymidine at position 3 in the dodecamer GT duplex is represented by (●).

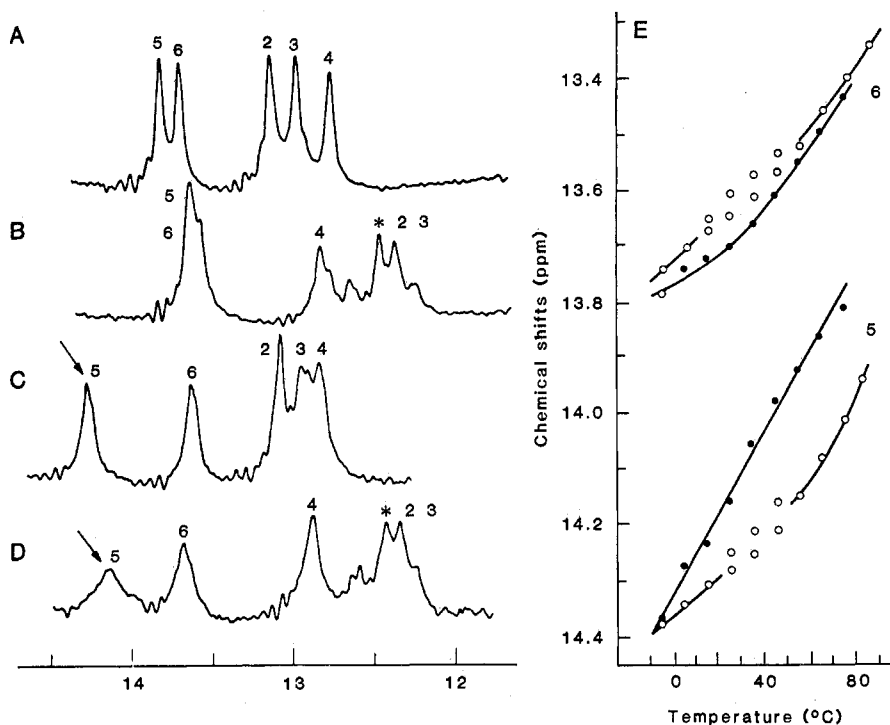


Fig. 7. The 360-MHz correlation proton NMR spectra (12 to 14.5 ppm) of (A) the dodecamer duplex, *pH* 6.80, (B) the two actinomycins per dodecamer complex, *pH* 6.75, (C) the one Netropsin per dodecamer complex, *pH* 6.89, and (D) the two actinomycins plus one Netropsin per dodecamer complex, *pH* 6.75, in 0.1*M* phosphate, 2.5 *mM* EDTA, 4:1 H<sub>2</sub>O:<sup>2</sup>H<sub>2</sub>O, at 27°C. The signal-to-noise ratios of the spectra were improved by applying a 5-Hz exponential line-broadening contribution. The upfield shifts of two guanosine H-1 imino protons on actinomycin binding are designated by an asterisk. The downfield shift at one thymidine H-3 imino proton on Netropsin binding is designated by an arrow. (E) Temperature dependence of the thymidine H-3 proton chemical shifts at base pairs 5 and 6 in (○) the one Netropsin per dodecamer duplex, *pH* 6.89, and (●) the two actinomycins plus one Netropsin per dodecamer complex in 0.1*M* phosphate, 2.5 *mM* EDTA, 4:1 H<sub>2</sub>O:<sup>2</sup>H<sub>2</sub>O solution.

## Antibiotic-d (CGCGAATTCGCG)

### Complexes

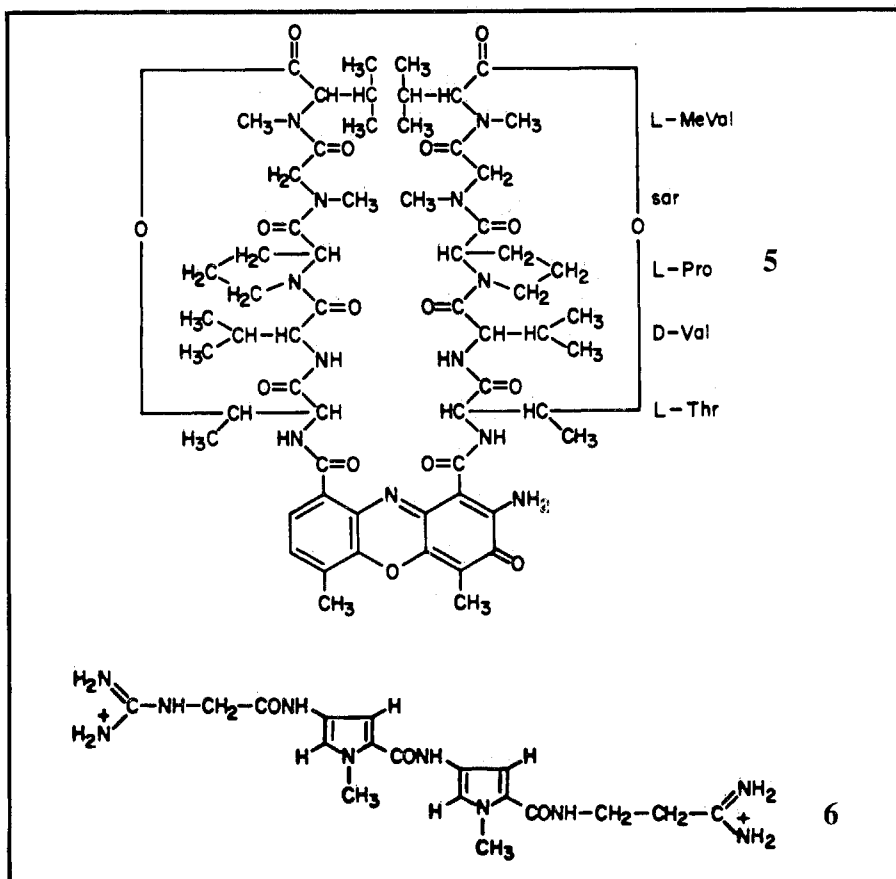
The mode of action of a large group of antibiotics, mutagens, and carcinogens involves complex formation with cellular DNA and inhibition of nucleic acid replication and expression (48, 49). The antibiotics in this series which do not bind covalently are sensitive probes of DNA conformation, and many of them have pronounced antitumor activity. Modern cancer chemotherapy treatments employ a combination of antitumor agents which act synergistically, and our efforts are addressed toward understanding this synergism at the molecular level.

Actinomycin (5) is an intercalating agent that exhibits a specificity for dG(3'-5')dC sites on duplex DNA (50, 51). The pentapeptide lactone rings of the antibiotic extend on either side of the phenoxazone chromophore, with the result that the antibiotic covers four to six base pairs centered about its intercalation site (52, 53).

Netropsin (6) is a groove binding peptide antibiotic which complexes preferentially in the minor groove of dA·dT-rich regions of duplex DNA (54-56). The complex is stabilized by hydrophobic, hydrogen bonding, and electrostatic interactions, with the antibiotic covering about three base pairs at its binding site (57).

There is one Netropsin binding site in the dA·dT tetranucleotide core and there are actinomycin binding sites at the flanking dG·dC tetranucleotide blocks at either end of the d(CGCGAATTCGCG) duplex. We have investigated the separate and simultaneous binding of the intercalating and groove binding antibiotics at adjacent sites on the dodecanucleotide duplex (58) to probe the degree of delocalization of the conformational changes associated with antibiotic binding and to search for mutual interactions between neighboring antibiotic binding sites.

**Actinomycin complex.** The imino proton spectrum of the five nonterminal base pairs of the dodecamer duplex at 27°C and their assignments are shown in Fig. 7A. We observe upfield shifts in the guanosine imino protons of the dodecamer on addition of two equivalents of actinomycin (designated by asterisks in Fig. 7B) along with removal of the two-fold element of symmetry in the complex. The upfield-shifted resonances at 12.3 to 12.5 ppm correspond to the guanosine imino protons of base pairs 2 and 3 adjacent to the dG<sub>2</sub>(3'-5')dC<sub>3</sub>, intercalation site (24, 59), while the slightly perturbed resonance at ~ 12.8 ppm cor-



responds to the guanosine proton of base pair 4. The thymidine imino protons of dA:dT base pairs 5 and 6 in the dodecamer duplex (Fig. 7A) undergo small upfield shifts on complex formation with actinomycin (Fig. 7B), demonstrating that addition of the intercalating antibiotics at the ends of the duplex perturbs the conformation at the center of the duplex.

Saturation recovery experiments on the actinomycin dodecamer complex show that the lifetimes of the thymidine imino protons decrease in the complex compared to the dodecamer duplex alone at 55°C (Table 4). This indicates that binding of actinomycin at the dG:dC sites slightly destabilizes the dA:dT base pairs in the dodecanucleotide duplex. Spectral titration and thermal denaturation studies had shown that actinomycin influenced the properties of the dG:dC binding region, as well as the dA:dT nonbinding region in the (dC<sub>15</sub>dA<sub>15</sub>)·(dT<sub>15</sub>dG<sub>15</sub>) complementary block copolymer (60).

**Netropsin complex.** The addition of one equivalent of Netropsin to the dodecamer duplex results in a large downfield shift of the thymidine imino proton of dA:dT base pair 5 (61) to 14.25 ppm (designated by arrow in Fig. 7C) while the thymidine imino proton of dA:dT base pair 6 shifts slightly to 13.6 ppm (Fig. 7C). There is a redistribution in the chemical shifts of the guanosine imino protons between 12.8 and 13.2 ppm on addition of Netropsin to the dodecamer duplex (compare Fig. 7, A and C) along with the removal of the twofold symmetry of the complex. The imino proton NMR data demonstrate that Netropsin binds at the dA:dT core of the dodecamer duplex and results in chemical shift perturbations at adjacent dG:dC regions. NMR (62) and electric field dichroism (63) measurements had shown that Netropsin induces a conformational change at its binding site on synthetic and natural DNA's which is propagated to adjacent antibiotic-free base pair regions.

Saturation recovery experiments on the Netropsin dodecamer complex indicate an increase in the duplex opening lifetimes of the thymidine imino protons of base pairs 5 and 6 by more than a factor of 3 on addition of Netropsin at 55°C (Table 4). These kinetic studies demonstrate that Netropsin binds to and stabilizes the dA:dT tetranucleotide core of the dodecamer duplex.

**Actinomycin and Netropsin complex.** The imino proton NMR spectrum of the dodecamer complex with two equivalents of actinomycin and one equivalent of Netropsin at 27°C is shown in Fig. 7D.

Table 4. Lifetimes (milliseconds) of the thymidine imino protons in the dodecamer duplex in the absence and presence of the antibiotics actinomycin and Netropsin in 0.1M phosphate, pH 7, 55°C.

| Antibiotic                          | Base pair 5 | Base pair 6 |
|-------------------------------------|-------------|-------------|
| None                                | 33          | 56          |
| Two actinomycins                    | 28*         |             |
| One Netropsin                       | 190         | 165         |
| Two actinomycins plus one Netropsin | 140         | 130         |

\*Resonances for base pairs 5 and 6 were superpositioned and hence only an average value could be estimated.

It exhibits the upfield shift of two guanosine imino protons characteristic of actinomycin intercalation at dG(3'-5')dC sites (24, 59) and the downfield shift of one thymidine imino proton characteristic of groove binding of Netropsin at dA:dT sites (61) on the dodecanucleotide duplex. These NMR results demonstrate that actinomycin and Netropsin can bind at adjacent dG:dC and dA:dT tetranucleotide blocks on the dodecamer duplex and support similar conclusions based on optical and hydrodynamic measurements of the simultaneous binding of these two antibiotics on block copolymers, natural and superhelical DNA's in solution (64).

The chemical shift difference between the thymidine imino proton of dA:dT base pair 5 in the Netropsin-dodecamer complex in the absence (Fig. 7C) and the presence (Fig. 7D) of actinomycin is maintained over a wide temperature range in the premelting transition region (Fig. 7E). This observed mutual interaction between adjacent intercalating and groove binding sites on the dodecanucleotide duplex receives support from the kinetic data obtained from saturation recovery measurements. We measure a slight decrease in the lifetimes of both thymidine imino protons in the Netropsin-dodecamer complex on addition of two equivalents of actinomycin D at 55°C (Table 4). Thus, the opening rates at the groove binding antibiotic site are perturbed by the presence of an intercalating agent at adjacent sites on the duplex.

**Phosphodiester markers.** The separate and simultaneous binding of actinomycin and Netropsin to the dodecamer duplex can also be monitored at the phosphodiester backbone of the duplex. This is based on the observed downfield phosphorus shifts on intercalation of actinomycin (24) and the upfield phosphorus shifts on groove binding of Netropsin (61) to the dodecamer duplex. The phos-

phorus NMR spectrum of the dodecamer complex with two equivalents of actinomycin and one equivalent of Netropsin exhibits the shifts characteristic of the simultaneous binding of the intercalating and groove binding antibiotics adjacent to each other along the duplex (58).

## Future Prospects

Our increased knowledge of DNA conformation represents a first step toward understanding the complementary structural surfaces and interactions involved in protein-DNA complexes. A second step toward this goal is to elucidate the interactions between smaller ligands such as antibiotics and DNA. This problem, which is of fundamental importance in its own right, has been addressed in this article and sets the stage for future investigations of the complex between the Eco RI restriction enzyme and methylase with its d(GAATTC) recognition site on the dodecanucleotide duplex in solution. NMR studies of this enzyme-DNA complex in solution should complement x-ray investigations of the complex in the solid state (65, 66).

## References and Notes

1. S. Arnott, R. Chandrasekaran, E. Selsing, in *Structure and Conformation of Nucleic Acids and Protein-Nucleic Acid Interactions*, M. Sundaralingam and S. T. Rao, Eds. (University Park Press, Baltimore, 1975), pp. 577-596.
2. S. Arnott and R. Chandrasekaran, in *Biomolecular Stereodynamics*, R. Sarma, Ed. (Adenine, New York, 1981), pp. 99-122.
3. V. Sasisekharan, M. Bansal, S. K. Bramachari, G. Gupta, in *Biomolecular Stereodynamics*, R. Sarma, Ed. (Adenine, New York, 1981), pp. 123-149.
4. K. Itakura, N. Katagiri, C. P. Bahl, R. H. Wightman, S. A. Narang, *J. Am. Chem. Soc.* **97**, 7327 (1975).
5. P. Dembek, K. Miyoshi, K. Itakura, *ibid.* **103**, 706 (1981).
6. M. A. Viswamitra, O. Kennard, P. G. Jones, G. M. Sheldrick, S. Salisbury, L. Falvello, Z. Shakked, *Nature (London)* **273**, 687 (1978).
7. A. H. J. Wang, G. J. Quigley, F. J. Kolpak, J. L. Crawford, J. H. van Boom, G. van der Marel, A. Rich, *ibid.* **282**, 680 (1979).
8. H. Drew, T. Takano, S. Tanaka, K. Itakura, R. E. Dickerson, *ibid.* **286**, 567 (1980).
9. D. J. Patel and L. L. Canuel, *Eur. J. Biochem.* **96**, 267 (1979).
10. P. S. Miller, D. M. Cheng, N. Dreon, K. Jayaraman, L. S. Kan, E. E. Leutzinger, S. M. Pulford, P. O. P. T'so, *Biochemistry* **19**, 4688 (1980).
11. T. A. Early, D. R. Kearns, W. Hillen, R. D. Wells, *Nucleic Acids Res.* **8**, 5795 (1980).
12. Abbreviations and conventions: C, cytidine; G, guanosine; A, adenosine; T, thymidine; U, uridine; d, deoxy; centered dot, as in dG:dC, refers to same base pair; hyphen as in dG-dC refers to adjacent bases on the same strand.
13. D. J. Patel, in *Peptides, Polypeptides, and Proteins*, E. R. Blout, Ed. (Wiley, New York, 1974), pp. 459-472.
14. D. R. Kearns, *Annu. Rev. Biophys. Bioeng.* **6**, 477 (1977).
15. D. J. Patel, *Acc. Chem. Res.* **12**, 118 (1979).
16. C. W. Hilbers, in *Biological Applications of Magnetic Resonance*, R. G. Shulman, Ed. (Academic Press, New York, 1979), pp. 1-43.
17. P. R. Schimmel and A. G. Redfield, *Annu. Rev. Biophys. Bioeng.* **9**, 181 (1980).
18. A. G. Redfield, S. Roy, V. Sanchez, J. Tropp, N. Figueroa, in *Biomolecular Stereodynamics*,

- R. Sarma, Ed. (Adenine, New York, 1981), pp. 195-208.
19. B. R. Reid, *Annu. Rev. Biochem.* **50**, 969 (1981).
  20. R. M. Wing, H. R. Drew, T. Takano, C. Broka, S. Tanaka, K. Itakura, R. E. Dickerson, *Nature (London)* **287**, 755 (1980).
  21. H. R. Drew, R. M. Wing, T. Takano, C. Broka, S. Tanaka, K. Itakura, R. E. Dickerson, *Proc. Natl. Acad. Sci. U.S.A.* **78**, 2179 (1981).
  22. D. J. Patel, S. Kozlowski, L. Marky, C. Broka, J. Rice, K. Itakura, K. Breslauer, *Biochemistry* **21**, 428 (1982).
  23. D. R. Kearns, D. J. Patel, R. G. Shulman, *Nature (London)* **229**, 338 (1971).
  24. D. J. Patel, *Biochemistry* **13**, 2396 (1974).
  25. — and C. W. Hilbers, *ibid.* **14**, 2651 (1975).
  26. R. E. Dickerson, H. R. Drew, B. Connor, in *Biomolecular Stereodynamics*, R. Sarma, Ed. (Adenine, New York, 1981), pp. 1-34.
  27. P. D. Johnston and A. G. Redfield, *Nucleic Acids Res.* **4**, 3599 (1977).
  28. —, *Biochemistry* **20**, 3996 (1981).
  29. R. E. Hurd and B. R. Reid, *J. Mol. Biol.* **142**, 181 (1980).
  30. D. M. Crothers, C. W. Hilbers, R. G. Shulman, *Proc. Natl. Acad. Sci. U.S.A.* **70**, 2899 (1973).
  31. H. Teitelbaum and S. W. Englander, *J. Mol. Biol.* **92**, 79 (1975).
  32. C. Mandal, N. R. Kallenbach, S. W. Englander, *ibid.* **135**, 391 (1979).
  33. T. A. Early, D. R. Kearns, W. Hillen, R. D. Wells, *Biochemistry* **20**, 3756 and 3764 (1981).
  34. V. Sanchez, A. G. Redfield, P. D. Johnston, T. Tropp, *Proc. Natl. Acad. Sci. U.S.A.* **77**, 5659 (1980).
  35. R. H. Sarma, C. K. Mitra, M. H. Sarma, in *Biomolecular Stereodynamics*, R. Sarma, Ed. (Adenine, New York, 1981), pp. 53-75.
  36. F. R. Prado, C. Giessner-Prettre, B. Pullman, *J. Mol. Struct.*, in press.
  37. D. J. Patel, *Biopolymers* **15**, 533 (1976).
  38. M. Guéron and R. G. Shulman, *Proc. Natl. Acad. Sci. U.S.A.* **72**, 3482 (1975).
  39. D. G. Gorenstein and D. Kar, *J. Am. Chem. Soc.* **99**, 672 (1977).
  40. D. J. Patel, L. L. Canuel, F. M. Pohl, *Proc. Natl. Acad. Sci. U.S.A.* **76**, 2508 (1979).
  41. D. J. Patel, S. A. Kozlowski, L. A. Marky, J. A. Rice, C. Broka, K. Itakura, K. J. Breslauer, *Biochemistry* **21**, 445 (1982).
  42. D. J. Patel and E. J. Gabbay, *Proc. Natl. Acad. Sci. U.S.A.* **78**, 1351 (1981).
  43. M. D. Topal and J. R. Fresco, *Nature (London)* **263**, 285 (1976); *ibid.*, p. 289.
  44. F. H. C. Crick, *J. Mol. Biol.* **19**, 548 (1966).
  45. D. J. Patel, S. A. Kozlowski, L. Marky, J. A. Rice, C. Broka, J. Dallas, K. Itakura, K. J. Breslauer, *Biochemistry* **21**, 437 (1982).
  46. S. Roy and A. G. Redfield, *Nucleic Acids Res.* **9**, 7073 (1981).
  47. D. R. Hare and B. R. Reid, *Biochemistry*, in press.
  48. E. F. Gale, E. Cundliffe, P. E. Reynolds, M. H. Richmond, M. J. Waring, *The Molecular Basis of Antibiotic Action* (Wiley, New York, ed. 2, 1981), chap. 5.
  49. S. Neidle, in *Progress in Medicinal Chemistry*, G. P. Ellis and G. B. West, Eds. (Elsevier, New York, 1979), pp. 151-220.
  50. J. Meienhofer and E. Atherton, *Adv. Appl. Microbiol.* **16**, 203 (1977).
  51. H. M. Sobell, *Prog. Nucleic Acids Res. Mol. Biol.* **13**, 153 (1973).
  52. W. Muller and D. M. Crothers, *J. Mol. Biol.* **35**, 251 (1968).
  53. M. J. Waring, *ibid.* **54**, 247 (1970).
  54. F. E. Hahn, in *Antibiotics III*, J. W. Corcoran and F. E. Hahn, Eds. (Springer-Verlag, New York, 1974), pp. 79-100.
  55. C. Zimmer, *Prog. Nucleic Acids Res. Mol. Biol.* **15**, 285 (1975).
  56. A. K. Krey, *Prog. Mol. Subcell. Biol.* **7**, 43 (1980).
  57. R. M. Wartell, J. E. Larson, R. D. Wells, *J. Biol. Chem.* **249**, 6719 (1974).
  58. D. J. Patel, S. A. Kozlowski, J. A. Rice, C. Broka, K. Itakura, *Proc. Natl. Acad. Sci. U.S.A.* **78**, 4063 (1981).
  59. T. A. Early, D. R. Kearns, J. F. Burd, J. E. Larson, R. D. Wells, *Biochemistry* **16**, 541 (1977).
  60. J. F. Burd, R. M. Wartell, J. B. Dodgson, R. D. Wells, *J. Biol. Chem.* **250**, 5109 (1975).
  61. D. J. Patel, *Eur. J. Biochem.* **99**, 369 (1979).
  62. — and L. L. Canuel, *Proc. Natl. Acad. Sci. U.S.A.* **74**, 5207 (1977).
  63. N. Dattagupta, M. Hogan, D. M. Crothers, *Biochemistry* **19**, 5998 (1980).
  64. R. M. Wartell, J. E. Larson, R. D. Wells, *J. Biol. Chem.* **250**, 2698 (1975).
  65. T. S. Young, P. Modrich, A. K. Seth, E. Jay, S. H. Kim, *J. Mol. Biol.* **145**, 607 (1981).
  66. J. M. Rosenberg and J. Grable, *ibid.*, in press.
  67. This research was undertaken in collaboration with S. Kozlowski (proton and phosphorus NMR), C. Broka (synthesis of oligonucleotides), and J. Rice (proton NMR). We are extremely grateful to H. Drew, R. Dickerson, and K. Breslauer for extensive discussions and information. We acknowledge the contribution of R. Sarma and his collaborators for undertaking the chemical shift calculations on the dodecanucleotide duplex. We used the high-resolution NMR facilities at the University of Pennsylvania Medical School (funded by NIH RR542), Caltech (funded by NSF CHE-7916324), the Stanford Magnetic Resonance Laboratory (funded by NSF GP23633 and NIH RR00711), the Francis Bitter National Magnet Laboratory, Massachusetts Institute of Technology (funded by NSF C-670 and NIH RR0095), and the University of California, Davis, NMR facility. We thank the operations managers of these facilities for their cooperation. We thank I. Tinoco of the University of California, Berkeley, for guidance, encouragement, and support during the kinetic measurements undertaken in his laboratory (supported in part by NIH GM10840 and DOE contract W-7405-EN6-48).

clearing of large areas of tropical forests could contribute to a global climate change.

Generalizations about the energy problems of developing countries and the solutions to them are difficult. These countries form a spectrum ranging from stagnating, abysmally poor countries to rapidly growing middle-income countries, like Korea and Brazil, with annual per capita incomes of \$1500 or more. The latter countries have such large and dynamic manufacturing sectors that they are close to being industrialized nations. At the other end of the spectrum are countries like Burundi and Upper Volta with per capita incomes of under \$200 a year. This wide variation in standards of living is reflected in the amounts of energy consumed. Per capita consumption of commercial energy in Korea, for example, is 60 to 80 times higher than it is in the above-mentioned African countries. So, although these countries share a common set of energy problems stemming mainly from their dependence on imported oil, they are affected by higher oil prices to different degrees, have different possibilities for solving their problems, and require different types of help.

The authors are senior fellows in the Center for Energy Policy Research at Resources for the Future, 1755 Massachusetts Avenue, NW, Washington, D.C. 20036.

## Energy and the Oil-Importing Developing Countries

Joy Dunkerley and William Ramsay

The oil-importing developing countries are a critical segment of the global energy, economic, and environmental scene (1, 2). Their oil imports currently represent some 5.5 million barrels per day (MBD) or 20 percent of the total oil exports of the Organization of Petroleum Exporting Countries (OPEC), but within 10 years their share is estimated to attain more than one-quarter of the total (3, 4). Indeed, from now to 1990, the oil-importing developing countries could account for all of the increase in demand for OPEC oil exports (5). What happens in these countries will therefore have a major impact on the course of oil prices, in which all importing countries, whether rich or poor, have a vital interest.

The ways in which the oil-importing developing nations finance these rising

oil imports also has an impact on the rest of the world. High levels of debt, made necessary to finance increasing import bills, threaten the stability of the international financial system. Alternatively, if the oil-importing developing countries are unable to afford more oil, their growth rate will suffer, threatening major export markets for the industrial countries and, ultimately, regional and global peace.

The linkage between the developing and the industrial world also extends to the developing countries' use of traditional fuels. Overuse of traditional fuels such as wood and crop and animal wastes can result in lowered agricultural productivity; loss of virgin tropical forest leads to extinction of plant and animal species; carbon dioxide emissions from